Energy and Buildings 158 (2018) 801–811

Contents lists available at ScienceDirect

Energy and Buildings

journal homepage: www.elsevier.com/locate/enbuild

Experimental investigation of double-pipe heat exchangers in air conditioning applications

Saud Ghani[a,*], Seifelislam Mahmoud Ahmad Gamaledin[a], Mohammed Mohammed Rashwan[a], Muataz Ali Atieh[b]

[a] Department of Mechanical Industrial Engineering, College of Engineering, Qatar University, P.O. Box 2713, Doha, Qatar
[b] College of Science & Engineering, Hamad Bin Khalifa University, Doha, Qatar

ARTICLE INFO

Article history:
Received 4 April 2017
Received in revised form 15 October 2017
Accepted 16 October 2017
Available online 18 October 2017

Keywords:
Double-pipe heat exchanger
Coefficient of performance (COP)
Energy consumption
Heating ventilating and air conditioning (HVAC)

ABSTRACT

The increased demand of energy in domestic applications necessitates the development of innovative engineering solutions in building heating, ventilating, and air conditioning (HVAC) systems. As the largest energy intensive sector is domestic buildings, more focus is currently directed to reduce air conditioning energy consumption. Double-pipe heat exchangers are considered one of the practical solutions in today's HVAC industry. Nevertheless, a few studies focus on using double-pipe heat exchangers in air conditioning applications. This paper experimentally investigates the usage of double-pipe condenser and evaporator in an air conditioning system serving a 45 m^3 balanced calorimeter of 2.24 kW heat load. Deionized water (DIW) was used as the secondary heat transfer working fluid for both the evaporator and condenser units, and R-22 was used as the AC system refrigerant. Experimental results of the double-pipe heat evaporator/condenser setup showed a promising reduction in the compressor work and an increase in the system coefficient of performance (COP). The collected data showed that the system efficiency depends more on the evaporator DIW flowrate than on the condenser DIW flowrate. By increasing the DIW flowrate in the evaporator, the compressor work was shown to decrease, while the COP was shown to increase. In comparison with a standard rated air conditioning unit, using a double-pipe evaporator and condenser units with the maximum DIW flowrates resulted in a decrease of about 53% in the compressor work and a similar percentage of increase in the system COP.

1. Introduction

The world population spends more than 90% of their time indoors [1,2]. Various studies showed that thermal comfort affects human health and work productivity [3–5]. The domestic energy demand represents approximately 20–40% of the total energy consumption in developed countries [6], surpassing other sectors such as industry and transport. Within the building sector, the highest power demand is for HVAC systems [7]. Recently, the demand for HVAC systems has grown as a result of globalization and the need for better thermal comfort environment [8]. For example, 87% of households have air conditioning equipment in the U.S. [9], and approximately 34% of the offices are equipped with central HVAC systems [10]. The growing reliance on HVAC systems in residential, commercial, and industrial environments has resulted in a huge increase in energy consumption, especially during the summer months [11]. The large difference in temperature between the indoor and outdoor environments during summer decreases the efficiency of air conditioning units [12].

The working principle of typical air conditioning systems is based on the vapor compression refrigeration cycle [13]. Depending on the working fluid, the air conditioning systems can be classified as follows: all-air systems, air-water systems, and unitary refrigerant-based systems [14]. In all-air systems, air is processed in the air conditioning plant and then conveyed to the conditioned space through insulated ducts by using blowers and fans. In air–water systems, both air and water are used for cooling the conditioned space. The air and water are cooled in a central plant and sent to the conditioned space. A room terminal unit, such as fan coil unit (FCU), an induction unit, or a radiation panel, is used to extract heat from the air-conditioned space. In all-water systems, chilled water is circulated to individual room terminal units. FCUs are then used to circulate the air within the room over the cold coil. Typically, chillers supply water at a temperature of approximately 6.67 °C, and the return water temperature is about 12.2 °C [15–18].

* Corresponding author.
E-mail addresses: s.ghani@qu.edu.qa (S. Ghani), seif.mahmoud@qu.edu.qa (S.M.A. Gamaledin), m.mohammed@qu.edu.qa (M.M. Rashwan), mhussien@qf.org.qa (M.A. Atieh).

https://doi.org/10.1016/j.enbuild.2017.10.051

HVAC systems' performance depends on their individual components' efficiency, operating conditions, and control strategies [19]. There is an opportunity for improvement in HVAC systems' efficiency through the hardware design of these systems [20]. Reviewing previous related research works identified various techniques that targeted one or more of these aspects to increase the efficiency and decrease the operational cost of HVAC systems. Many studies focused on the enhancement techniques of the system's heat exchangers. These methods can be classified into active, passive, and compound methods [21]. The active methods use an external power for increasing the heat transfer rate and are more complex from the use and design points of view. However, the passive methods do not require an external power to enhance heat transfer and promote higher heat transfer coefficients by disturbing or altering the existing flow behavior. The compound method is where more than one of the above techniques is used in combination. To optimize the overall performance of the HVAC systems and decrease their energy consumption, the thermal performance of the evaporator and the condenser, which are the main heat-exchanging units, can be enhanced using one or more of these methods.

1.1. Double-pipe heat exchangers

Double-pipe heat exchangers, also known as double-tube, double-duct, or tube-in-tube heat exchangers, are considered one of the devices for passive heat transfer enhancement. In double-pipe exchangers, one fluid flows inside a pipe, and the other fluid flows in the vicinity between the outer pipe and the inner pipe [22–24]. This is also referred to as a concentric tube construction and considered one of the most simple and applicable heat exchangers [25]. The theory behind the operation of a double-pipe heat exchanger was discussed in detail by F.P. Incropera [26]. Various double-pipe heat exchanger working fluid characteristics and performance enhancement abilities were discussed by several researchers [27–29]. Others studied the characteristics of double-pipe geometry and configuration [30–32], while some researchers focused on other heat transfer enhancement methods [33–37]. Omidi et al. [25] provided a comprehensive review of double-pipe heat exchangers.

Double-pipe heat exchangers are used in many industries because of their low design and maintenance costs, flexibility, and low installation costs [25]. They are mainly used for sensible heating or cooling of process fluids in applications of small heat transfer areas of up to 50 m^2 [38]. The configuration is also suitable for high-pressure fluids and high fouling conditions because of the ease of their maintenance and cleaning [24]. Nevertheless, their major disadvantage is their bulky design and the cost per unit transfer surface.

Depending on the pipe configuration, double-pipe heat exchangers are classified into straight coiled pipes and helical coiled pipes [24]. Helical coiled double-pipe heat exchangers are considered the most applicable type of heat exchangers in various industries including cooling applications because of their high performance, high heat transfer rate, and compact volume.

Flow in a double-pipe heat exchanger can be co-current or counter-current [39]. Double-pipe heat exchangers are usually used as counter-current heat exchangers and can be considered as alternatives to shell-and-tube heat exchangers. The friction factor and the heat transfer coefficient are the major parameters to be considered in the design of double-pipe heat exchangers. Furthermore, they have four key design components: shell nozzles, tube nozzles, shell-to-tube closure, and return-bend housing [24]. The outer pipe is commonly designed with an inner diameter in the range 50–400 mm and a nominal length in the range 1.5–12.0 m per hairpin. The outer diameter of the inner tube may vary between 19 and 100 mm [24].

Several studies have evaluated the experimental performance of double-pipe heat exchangers by using different heat transfer fluids such as nanofluids. Nevertheless, different numerical attempts have been made to evaluate the performance of double-pipe heat exchangers in both steady and transient states. The complexity of the double-pipe heat exchanger design, especially their geometry and fluid flow patterns, puts several solution constrains without assuming strict simplifications and assumptions [40,41]. For example, F.P. Incropera [26] obtained the derivation of the transient behavior with respect to heat transfer. The author showed that the value of heat transfer changes with a continuous change in pipe conditions such as inlet temperature, flowrate, fluid properties, and fluid composition. This transient behavior leads to changes in process temperatures, which results in a point where the temperature distribution becomes steady. The fluid temperature changes when the heat transfer begins. Until the temperature reaches a steady state, the behavior is dependent on time, which is a complex process to analyze.

Although double-pipe heat exchangers are currently used in many industries, their use in air conditioning applications has not been fully explored. The most relevant study was conducted by Rakesh and Manjunath [42] by using a modified laboratory-scale refrigeration system by incorporating a double-pipe heat exchanger in between the condenser and the expansion valve. That study reported an increase in the system COP by almost 50%. The authors also carried out CFD simulation, which was validated by the experimental results. Balaji et al. [43] performed experiments on a domestic air conditioning system equipped with a shell-and-coil-type heat exchanger as an intercooler. Using different nanofluids of different concentrations and flowrates, the authors concluded a maximum COP enhancement of 49.32%. Parameshwaran and Kalaiselvam [44] investigated possible improvements in the thermal performance and energy efficiency of an air conditioning system chiller using silver nanoparticles. The authors concluded their study with a potential daily maximum energy savings of 51%. Yau [45] developed an empirical model for the HVAC system of an operating theatre to test the design of a double-pipe heat exchanger in the air handler unit. The author concluded that the double-pipe heat exchanger design would consume a power of 51,000 kWh/year, which is lesser than that consumed by the typical existing system. The author attributed this to the redistribution of the cooling capacity within the HVAC system. Nevertheless, the author noted the drawback of the additional fan power needed to overcome the pressure drops associated with the additional tubes.

In this study, the performance of a novel vapor compression refrigeration cycle air conditioning system equipped with double-pipe heat exchangers is presented. Ultimately, the objective of this study is to assess the thermal and energy performance enhancement when using double-pipe evaporator and condenser in domestic air conditioning applications.

2. Experimental investigation

The experimental setup, testing schemes, data collection, and calculation procedures were performed in accordance with the current standards [46–48]. Testing standards were considered to establish a unified testing method and specify the types of testing equipment and data required in addition to the calculations and testing procedures [46–48]. Nine different experiments were conducted with different evaporator and condenser DIW flowrates.

2.1. Testing standards and requirements

The standards specify various testing methods and procedures to determine the specifications of room air conditioners [49]. By

Table 1
Major requirements and test conditions set by different international testing standards.

Testing standard	Types of testing calorimeters	Outdoor testing temperature (°C)		Indoor testing temperature (°C)		Data to be reported for cooling capacity tests
		DB	WB	DB	WB	
ISO 5151: 2010	Balanced ambient room and calibrated room calorimeters	35	24	27	19	Total cooling capacity (W), Sensible and latent cooling capacities (W), Indoor side air flowrate (L/s), and Effective power input to equipment (W)
ANSI/ASHRAE Standard 16–2016	Balanced ambient room and calibrated room calorimeters	35	23.9	26.7	19.4	Cooling and dehumidification (W), Flowrate (L/s), Current (A), and Power input (W)
AHRI Standard 340/360: 2015	Balanced ambient room and calibrated room calorimeters	35	24	27	19	Cooling and dehumidification capacities (W), Flowrate (L/s), Current (A), and Power input (W)
Jamaican DJS 179: 2016	Balanced ambient room and calibrated room calorimeters	35	23.9	26.7	19.4	Cooling capacity (W), EER, Indoor side air flowrate (L/s), and Power input (W)

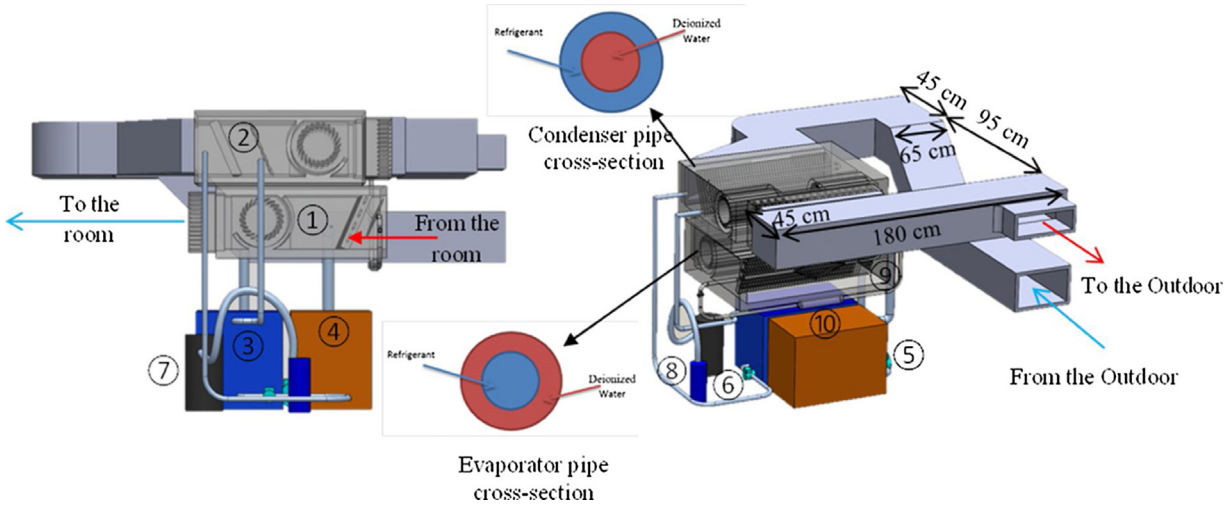

Fig. 1. Experimental setup and the unit components.

implementing these testing standards, the comparison and evaluation of different models of room air conditioners are possible. The specified testing procedures do not inhibit innovations or prevent improvement in design and performance [50]. Rating an air-conditioning system begins with the selection of a proper testing standard according to its type. The standard will dictate the selection of the room calorimeter and the airflow measuring equipment. Hence, testing and calculation of ratings are in accordance with the appropriate methods [46].

Calorimeters provide a controlled environment for determining the cooling capacity on the room side alone or preferably on the outdoor side as well. There are two types of room calorimeters: the balanced ambient room and the calibrated room calorimeters [46,51]. The main difference between the psychometric and balanced calorimeters is that the calculation and measurement methods with the balanced room have less measurement uncertainties because of the lower number of required parameters and measuring instruments [51]. In addition, the outdoor-side compartment in the balanced calorimeter does not require additional enclosure for balanced ambient operation when only the indoor room-side capacity test method is used. The ISO [48] tabulated the required sizes for calorimeters according to the rated cooling capacity of the equipment.

For air conditioning system rating tests, the international standards set the measurement techniques and the minimum requirements for instrumentation. For example, the Air-conditioning, Heating, and Refrigerating Institute (AHRI) stated that all dry bulb (DB) and wet bulb (WB) temperatures should be measured using an instrument with accuracy $\leq \pm 0.2\,^{\circ}C$ and a display resolution of $\leq 0.1\,^{\circ}C$. The ISO [48] adopted similar limits and added the uncertainties of other parameters such as time, mass, speed, and electrical input.

When testing air conditioning systems, three international climate conditions can be used: moderate climate, cool climate, and hot climate [47,48]. The moderate climate represents an outdoor DB air temperature of $35\,^{\circ}C$ and a WB air temperature of $24\,^{\circ}C$, maintaining an indoor DB temperature of $27\,^{\circ}C$ and a WB temperature of $19\,^{\circ}C$. Similar temperature testing conditions were used to investigate the intercooler effect on a domestic air conditioning system [43]. Table 1 summarizes the major test requirements and conditions for the major international testing standards. For each standard, the table presents the type of required testing calorimeter, the outdoor and indoor DB and WB temperatures, and the required reported data.

The cooling capacity (W) and COP values are among the typically published ratings for commercial domestic and industrial air conditioning equipment (AHRI 2015). The cooling capacity is the amount of sensible and latent heat that the equipment can remove from the conditioned space in a defined interval of time and is expressed in Watts (ISO 2010). The net cooling capacity is associated with the change in air enthalpy between the air entering and leaving the unit as represented by Eq. (1).

$$Cooling\ \ Capacity\,(W) = (Roomair\ Enthalpy - Suppl\ yair\ Enthalpy) \quad (1)$$

The COP is the ratio of the cooling capacity to the effective power input to the device at any given set of rating conditions [48]. The

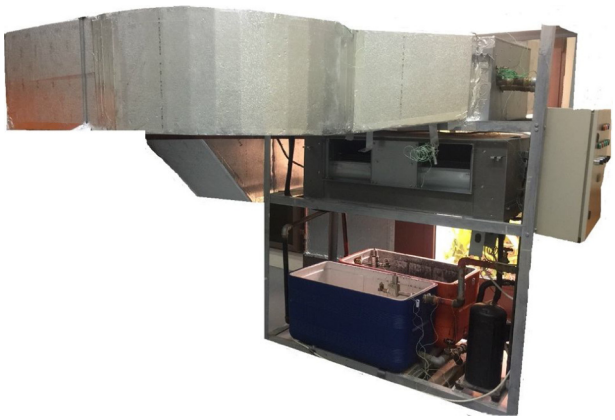

Fig. 2. Front side of the actual air conditioning unit experimental setup.

mathematical representation of COP is shown in Eq. (2). Typical air conditioning units have COP values between 2.3 and 3.5 [13].

$$COP = \frac{Cooling\ \ capacity\,(W)}{Power\ input\,(W)} \tag{2}$$

2.2. Experimental setup

An air conditioning system of 17.7 kW cooling capacity was developed using double-pipe evaporator and condenser in the present experimental study. The system runs on a standard vapor compression refrigeration cycle and consists of four major components: an evaporator, a condenser, capillary tubes, and a compressor. The evaporator and the condenser units used in this system are of double-pipe heat exchanger type, in which the refrigerant is allowed to exchange heat with the running DIW in addition to ambient air. In the evaporator unit, R-22 refrigerant runs in the inner pipe, while the DIW runs in the outer pipe, and in the condenser unit, R-22 refrigerant runs in the outer pipe, while the DIW runs in the inner pipe. Both the refrigerant and the DIW run in a co-current flow configuration where the two fluids flow in a parallel direction. The components of the double-pipe air conditioning unit and the evaporator and the condenser pipes' cross-sections with the refrigerant and DIW flow arrangement are illustrated in Fig. 1. The experimental setup is presented in Fig. 2.

The air conditioning unit is vertically configured where the evaporator unit is positioned below the condenser unit. Two 150-L DIW foam-insulated tanks and two small circulation pumps are fitted to supply the double-pipe evaporator and condenser with DIW from each tank. The unit is also equipped with a 5.2 kW compressor, a filter drier, an accumulator, and capillary tubes. The condenser intake and exhaust ducts are made of preinsulated aluminum phenolic foam sheets of 20-mm thickness and sealed to prevent air leakage. The ducts are connected to the condenser air inlet and exit sides to channel air in and out of the unit. Table 2 lists the specifications of the air conditioning system components.

For the rated air conditioning system cooling capacity of 17.7 kW, the required calorimeter geometry is 3.5 m × 2.4 m × 4.9 m width × height × length [48]. As shown in Fig. 3, the balanced calorimeter consists of an indoor-side compartment and an outdoor-side compartment. The outdoor-side compartment does not require an additional enclosure to balance ambient operation when only the indoor room-side capacity test method is used [46]. A similar setup was used to test two air conditioner types in different balanced calorimeter sizes [51]. Fig. 3 also shows the additional outer shell developed around the calorimeter to provide proper insulation for the testing calorimeter.

To provide proper insulation for the experimental setup, the air conditioning unit was placed in a calorimeter room. The wall behind the air conditioning unit, through which the condenser ducts pass, and the top of the conditioned space were made of concrete. An insulation cladding of 6-mm-thick plywood partitions was built around the calorimeter room.

Table 5
Evaporator and condenser DIW flowrates used in the experiment.

Flowrate	Evaporator (kg/s)	Condenser (kg/s)
Low	0.01	0.003
Medium	0.02	0.007
High	0.04	0.01

Temperature sensors were located at each air inlet and outlet. DIW flowmeters and temperature sensors were positioned at the DIW tanks. All sensors were then connected to a FLUKE HYDRA series II data logger. A FLUKE 434 Energy Analyzer was used to measure the energy consumption of different equipment including the compressor, evaporator fan, condenser fan, and the two DIW circulation pumps at all times. Fig. 4 shows the schematic diagram of the system components and sensor positions, and Table 3 lists the specifications of the measuring equipment.

The instrumentation specifications are listed in Table 3.

2.3. Experimental procedures

The air conditioning unit test procedure consists of three phases: a preconditioning period, an equilibrium period, and a data collection period (ISO 2010). The air conditioning unit must be operated until equilibrium conditions are maintained for not less than 1 h before capacity test data are recorded. The data collection commences when the measurements recorded during the equilibrium period reach an uncertainty limit of 0.2 °C for DB and WB temperatures and 5% for volume flowrate.

The outdoor air was introduced at a 35 °C DB temperature and 24 °C WB temperature. The indoor-side compartment was heated up to a temperature of 35 °C by using three heaters of 2.24 kW each. Two heaters were switched off once they reached the standard conditions, and the remaining heater was kept on to simulate the average heat loads within the conditioned space. The average total heat load per person doing moderately active office work is about 132 W [52]. The average load density of an office of a medium load with 8 computers, 8 screens, 1 laser printer, and 1 fax machine is about 929 W [53]. In addition, the heat load generated by the compartment lights was approximately 262.5 W at a rate of 20 W/m^2. Hence, the total heating load within the calorimeter room was 2.24 kW. Table 4 shows a summary of the reprehensive individual heat sources and the total heat load within the calorimeter room.

When equilibrium was achieved in the calorimeter room, the evaporator and condenser DIW pumps, evaporator and condenser fans, and the compressor were switched on to start the air conditioning process. Using the data acquisition and the energy analyzer devices, the sensor readings and energy data were recorded at every 5-s intervals. The evaporator and the condenser DIW flowrates were varied to investigate the effect of changing the DIW flowrates and to identify the optimum DIW flowrate for each heat exchanger. The DIW flowrate values were measured using two KOBOLD flowmeters positioned at the return of each DIW tank. The DIW pumps feeding the evaporator and condenser were of different flowrate capacities. As the DIW tanks were larger than required for low DIW flowrates, the DIW temperature values recorded at both the suction and return streams were almost identical. Table 5 shows the three different evaporator and condenser DIW flowrates used in the experimental work: low, medium, and high flowrates.

Because the condenser and evaporator pumps used were of a small DIW flowrate difference margin, nine experimental combinations of different evaporator and condenser DIW flowrates were

Table 2
List of equipment and their specifications for air conditioning system.

Compressor		Condenser Pump		Evaporator Pump		Accumulator		Filter Drier	
Model	Copeland	Model	GRUNDFOS Selectric	Model	NOCCHI	Model	Virginia KMP	Model	Emerson
Type	ZR72KC-TFD	Type	UPS 15–50	Type	SR3 25/50 180	Type	VA-57-7SRD	Type	EK-163S
Power	5.2 kW	Flow, Q:	Max. 3.3 m^3/h	Flow, Q:	Max. 3.6 m^3/h	Liquid holding capacity	9.5 LBS	Filtration	20 μm
Current	8.8 A	Head, H:	Max. 6 m	Head, H:	Max. 5.4 m	Flow capacity	25.7 at +4 °C 16.7 at −6 °C 11.4 at −17 °C	Maximum working pressure	680 psia
Mass Flowrate	0.111 kg/s.	Liquid temp.:	+2 to +95 °C	Liquid temp.:	+10 to +110 °C	Safe working pressure	21 bar	Type	Compacted bead filter
Refrigerant	R-22 HCFC	Power for each of the 3 speeds	0.17 A, 40 W 0.28 A, 70 W 0.42 A, 105 W	Power for each of the 3 speeds	0.26 A, 56 W 0.35 A, 78 W 0.45 A, 104 W	Compatibility	CFC, HCFC and HFC compatible	Fluids	Moisture and acids
Cooling Capacity	17.7 kW	Frequency	50 Hz	Frequency	50 Hz	Applications	Air Conditioning and heat pumps applications	Applications	Refrigeration
References	http://www.emersonclimate.com	References	http://www.grundfos.com/	References	http://www.nocchi.it	References	http://www.att-spares.de	References	http://www.emersonclimate.com

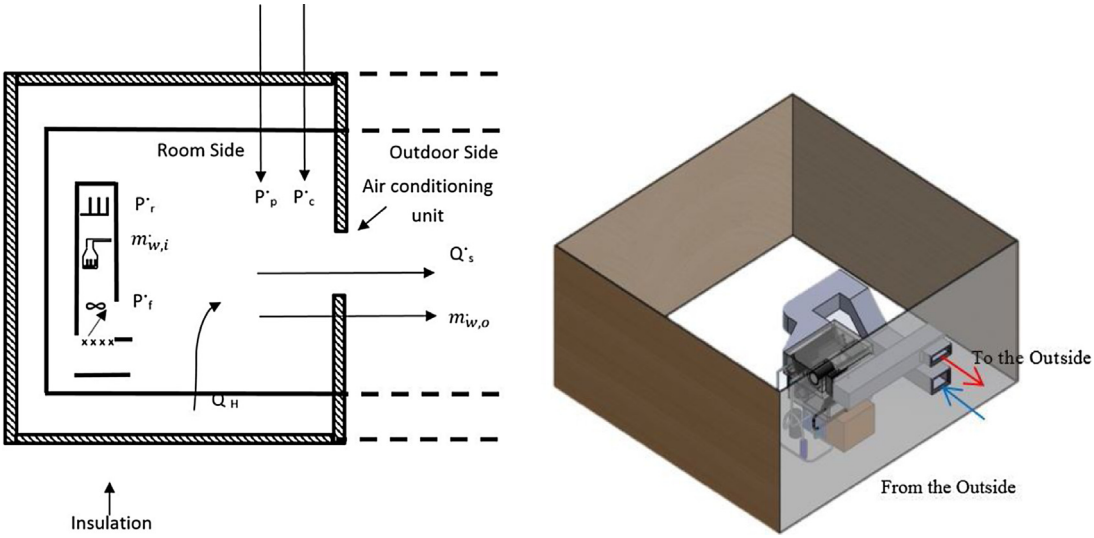

Fig. 3. Schematic of balanced calorimeter and the outer shell.

selected. Table 6 shows the experimental sets that were conducted in this study. The compressor rated cooling capacity and power consumption values were considered the benchmark case. Furthermore, to evaluate the thermal performance of the double-pipe evaporator and condenser in the air conditioning unit, different DIW flowrates of the double-pipe evaporator and condenser were used.

For each experiment, the Reynolds number of the evaporator and condenser DIW flow was calculated. The condenser DIW flow was shown to be distributed between laminar and transient flows, while 78% of the experiments were conducted with a turbulent or transient evaporator DIW flow. The DIW flow in the condenser had a Reynolds number in the range 775–2540, while that in the evaporator had a Reynolds number in the range 2540–10161. The evaporator DIW Reynolds number values were generally greater than the condenser values because the DIW runs in the outer pipe, which has a larger diameter than the condenser, in which the DIW runs in the inner pipe. Furthermore, the flowrate in the evaporator secondary fluid pump was higher than that in the condenser secondary fluid pump, thus resulting in a flow with higher velocity range in the pipe.

3. Experimental results

During the indoor air capacity test, the data recorded included the test date and time, input power, evaporator supply air velocity, condenser intake and exhaust air velocities, and DB and WB temperatures of air entering and leaving the air conditioning equipment (ISO 2010). By using the data acquisition system, the data were collected every 5 s from the different sensors fixed to the air conditioning unit. Fig. 5 depicts the typical results of DB and WB temperature profiles, for both room and supply, versus the experimental time for Experiments 1 and 3 because they represent the worst and the best system performance cases, respectively. In Fig. 5(a) and (b), the x-axis shows the experimental time in seconds, the primary y-axis shows the DB temperature (°C), and the secondary y-axis shows the WB temperature (°C).

Fig. 5 shows that the average supply air temperature was approximately 22 °C in all the experiments, as presented in Table 6, except in experiment 1, where both evaporator and condenser DIW pumps were switched off. Thus, the DIW was stagnant in the void between the double-pipe heat exchangers. Furthermore, the air conditioning unit managed to lower the room DB temperature by

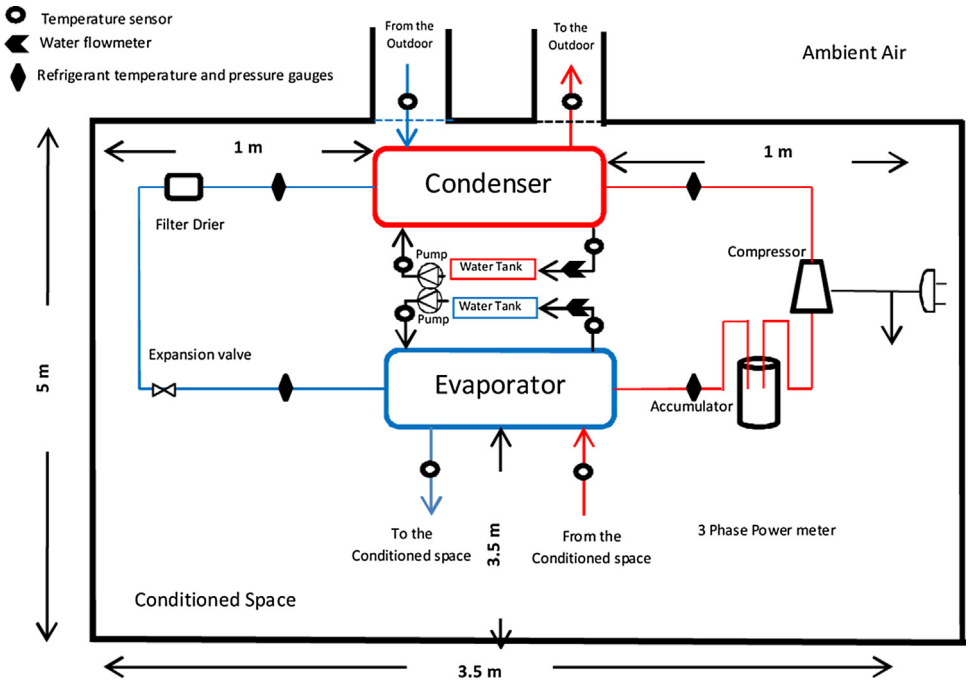

Fig. 4. Locations of different sensors within the air conditioning unit.

Table 3
Instruments and their specifications.

Fluke 434 energy analyzer		FLUKE HYDRA series II data logger		P&M replacement pressure gauges	
Measurement methods	IEC61000-4–30 class A	Measurement methods used	IEC 1010-1, ANSI/ISA S82.01-1994, CSA-C22.2 No. 1010.1-92, and EN61010-1:19	UPC No.	20032
Voltage measurement accuracy	±0.5% of nominal voltage	Voltage measurement accuracy	0.29% + 0.25 V	Item No.	FRGLGF
Voltage measurement resolution	0.1 Vrms	Voltage measurement resolution	10 mV	Low pressure range	−30-0-250 psi
Voltage measurement range	1–1000 Vrms	Voltage measurement range	1–300 Vrms	High pressure range:	−30-0-500 psi
Power measurement accuracy	±1.5% ± 10 counts	Temperature measurement accuracy for type K thermocouples	±0.43 °C	Refrigerants	R22, 134a, 404
Power measurement resolution	0.1–1 kW	Repeatability	3 ms for the Specified Conditions	Connections	1/4" SAE back connection, 2–3/4" (70 mm) O.D.
Power measurement range	1.0–20.00 MW	Frequency range	15 Hz to greater than 1 MHz	Others	Oil filled
Operating temperature	0 °C–+50 °C battery only, 0 °C–+40 °C with adapter	Operating temperature	0 °C–60 °C		
Reference	http://us.flukecal.com	Reference	http://us.flukecal.com	Reference	http://www.pnm-hvacr.com

Table 4
Calorimeter room heat loads considered in the experiments.

Heat source	Number	Each (W)	Diversity	Total heat load (W)	Reference
Person doing moderately active office work	8	131	1	1048	[52]
Computer	8	65	0.75	390	[53]
Monitors	8	70	0.75	420	[53]
Laser printer-desk	1	215	0.5	108	[53]
Fax machine	1	15	0.75	11	[53]
Lighting	17.5 m^2	20 W/m^2	0.75	262.5	Measured
Total				2240 (W)	

about 10 °C in all the experiments, except in experiment 1. The maximum temperature drop recorded in experiment 1 was about 7 °C, and hence, the temperature of the supply air remained constant. This could be attributed to the external frost formed on the evaporator pipes and the subsequent loss of heat transfer on the outdoor side compartment (Fig. 6).

Table 6
Experimental studies and corresponding evaporator and condenser flowrates.

Experiment	Evaporator DIW Flowrate	Condenser DIW Flowrate	Remarks
Experiment 1	Zero	Zero	Both pumps switched off
Experiment 2	Low 0.01 (kg/s)	Low 0.003 (kg/s)	Low DIW flowrate for both heat exchangers
Experiment 3	High 0.04 (kg/s)	High 0.01(kg/s)	High DIW flowrate for both heat exchangers
Experiment 4	Zero	High 0.01(kg/s)	Fixed condenser DIW flowrate
Experiment 5	Low 0.01 (kg/s)	High 0.01(kg/s)	
Experiment 6	Medium 0.02 (kg/s)	High 0.01(kg/s)	
Experiment 7	High 0.04 (kg/s)	Zero	Fixed evaporator DIW flowrate
Experiment 8	High 0.04 (kg/s)	Low 0.003 (kg/s)	
Experiment 9	High 0.04 (kg/s)	Medium 0.007 (kg/s)	

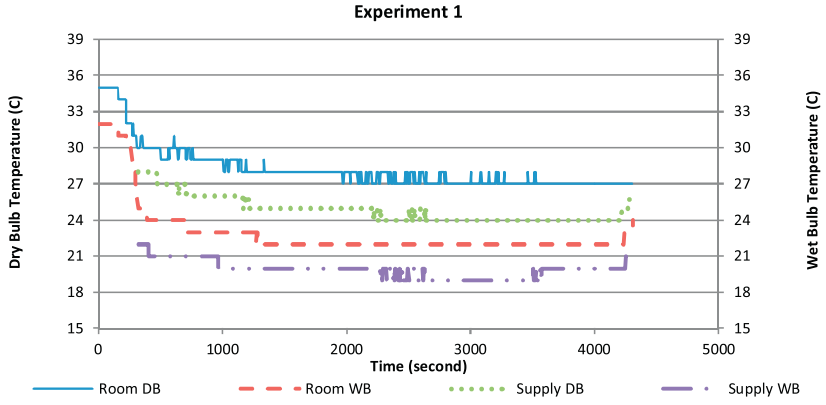

a) Experiment 1 room and supply DB and WB temperature profiles versus experimental time.

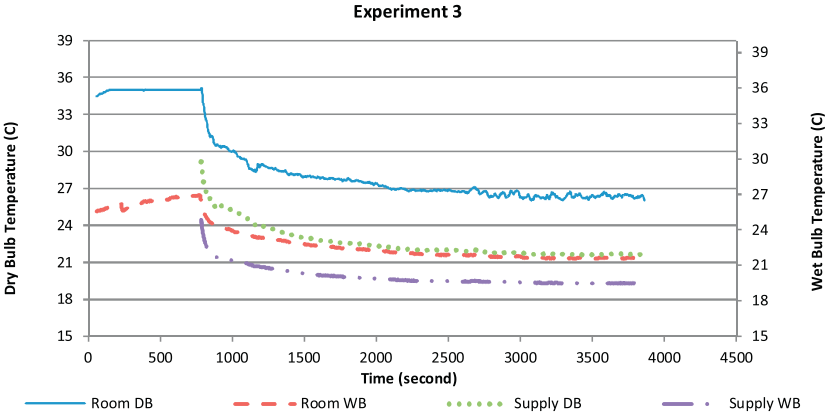

a) Experiment 3 room and supply DB and WB temperature profiles versus experimental time.

Fig. 5. Room and supply DB and WB temperatures versus experimental time.

Table 7
Different refrigeration parameters as a result of changing evaporator DIW flowrate.

Measured Values									Calculated Values		
Experiment No.	Evaporator DIW Flowrate	T_1 (°C)	T_2 (°C)	T_3 (°C)	T_4 (°C)	Evaporator Pressure (bar)	Condenser Pressure (bar)	Current (Amp.)	Compressor Work (kJ/Kg)	Cooling Effect (kJ/Kg)	COP
Experiment 4	Zero	−3.8	65.5	31	−4.5	N/A	N/A	N/A	N/A	N/A	N/A
Experiment 5	Low	7	65	38	6	16.5	6.5	7.1	30.3	160.2	5.3
Experiment 6	Medium	6	63	35	5	16.2	6.3	6.8	29.225	163.7	5.6
Experiment 3	High	5.2	56	33	4	15.86	6.1	6.7	22	166	7.5

Table 8
Different refrigeration parameters as a result of changing condenser DIW flowrate.

Measured Values									Calculated Values		
Experiment No.	Condenser DIW Flowrate	T_1 (°C)	T_2 (°C)	T_3 (°C)	T_4 (°C)	Evaporator Pressure (bar)	Condenser Pressure (bar)	Current (Amp.)	Compressor Work (kJ/kg)	Cooling Effect (kJ/kg)	COP
Experiment 7	Zero	6	67	38	5	17.1	6.5	7.4	31.05	160.2	5.2
Experiment 8	Low	5	63	35	4	16.9	6.3	7.2	28.5	163.7	5.7
Experiment 9	Medium	5	60	34.2	4	16.55	6.3	6.9	26.2	165	6.3
Experiment 3	High	5.2	56	33	4	15.86	6.1	6.7	22	166	7.5

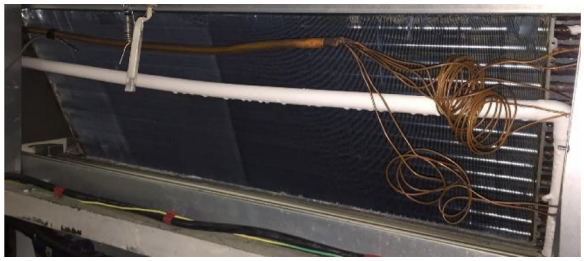

Fig. 6. External frost formed on the evaporator double pipe.

For each experiment, the thermodynamic refrigeration cycle was plotted on a pressure–enthalpy (P–h) diagram using the measured temperature and pressure values. The actual sensible heat removed by the air conditioning unit's refrigerant was then calculated from the refrigeration cycle. Table 7 presents different refrigerant conditions, calculated compressor work, produced refrigeration effect, and system COP as a result of changing the evaporator DIW flowrate while keeping the condenser DIW flowrate at its maximum. It should be noted that Experiment 4 in Table 7 was excluded from the analysis because the frost formed on the evaporator pipes stopped the experiment. Table 8 shows the same parameters under the effect of changing the condenser DIW flowrate, while keeping the evaporator DIW flowrate at its maximum. The experiments in Tables 7 and 8 are listed according to the evaporator and condenser DIW flowrates, respectively.

In Tables 7 and 8

T1 is the refrigerant temperature at the evaporator outlet and compressor inlet

T2 is the refrigerant temperature at the compressor outlet and condenser inlet

T3 is the refrigerant temperature at the condenser outlet and capillary tube inlet

T4 is the refrigerant temperature at the capillary tube outlet and evaporator inlet

The P–h diagram was plotted for Experiment 3 by using the thermodynamic operating points of the refrigeration system because it yielded the highest percentage improvement in compressor work and COP among the rated values. Fig. 7 shows

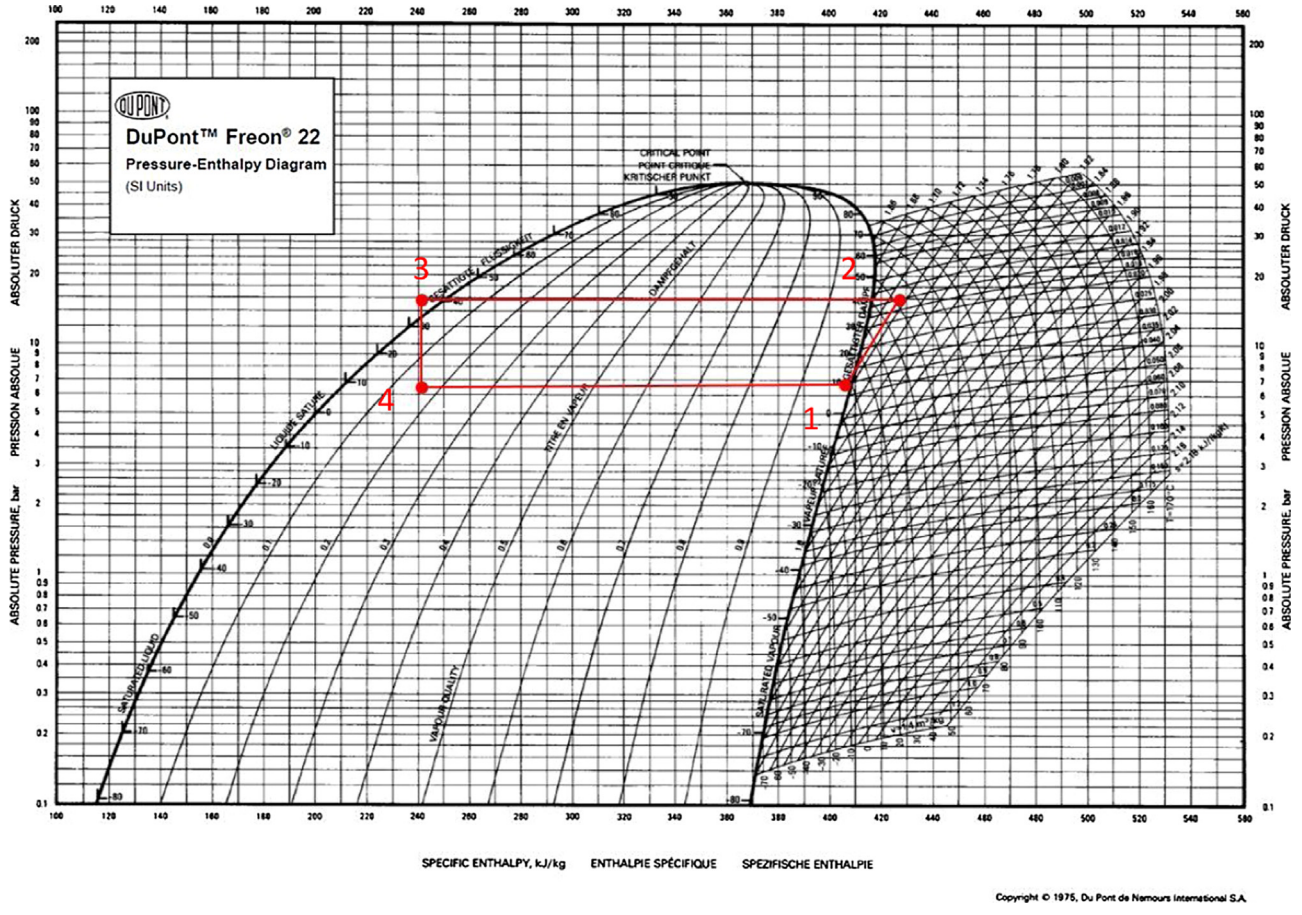

Fig. 7. P–h diagram of Experiment 3.

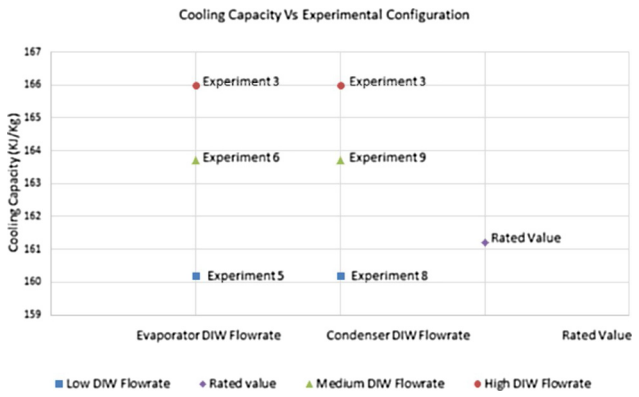

Fig. 8. Cooling capacity versus experimental configuration.

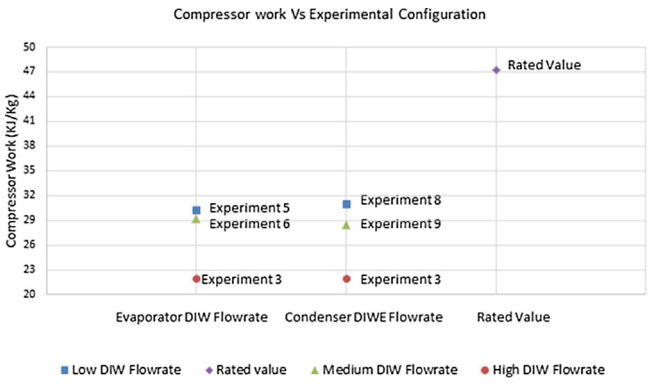

Fig. 9. Compressor work versus experimental configuration.

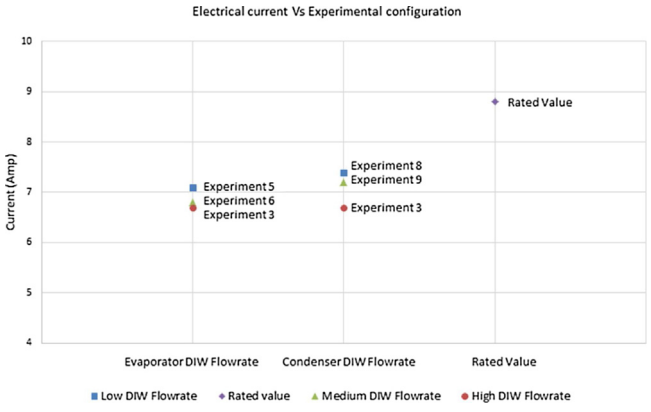

Fig. 10. Total operating electric current versus experimental configuration.

the P–h diagram of Experiment 3 based on the listed values in Tables 7 and 8.

The time required to achieve the set point temperature in the calorimeter room was measured using the collected data from the data logging instrument. As shown previously in Fig. 5, the required temperature drop was achieved in all the experiments, except in Experiment 1, where limited heat transfer occurred, which was caused by the external frosting on the evaporator tubes, and hence, it was excluded from the analysis. By recording the time required to reach the room set temperature, a higher dependence on the evaporator flowrate than that on the condenser flowrate was observed. There was a nearly constant time taken by the air conditioning unit to reach the set temperature despite the change in the condenser DIW flowrates. However, changes in the evaporator DIW flowrates in Experiments 4–6 had a greater effect on the time required by the air conditioning unit to reach the same set temperature. A minimum experimental time of 14 min was recorded for Experiment 7, while a maximum time of 33 min was recorded for Experiment 3 for the room to reach the set temperature.

3.1. *Effect of DIW flowrate*

Variations in the evaporator and condenser DIW flowrates affected the system cooling capacity, compressor work, total operating electric current, and system COP. As presented in Table 6, seven experiments were run with either higher evaporator DIW flowrate or higher condenser DIW flowrate. Experiment 3 was run with a high DIW flowrate for both the evaporator and the condenser. Experiments 4–6 were run with a high condenser flowrate against no DIW flowrate, low DIW flowrate, and medium DIW flowrate at the evaporator. Experiments 7–9 were run with a high evaporator DIW flowrate against no DIW flowrate, low DIW flowrate, and medium DIW flowrate at the condenser. Experiment 4 was excluded from the analysis because the frost formed on the evaporator pipes stopped the experiment.

Fig. 8 shows the effect of changing the evaporator and condenser DIW flowrates on the cooling capacity. Compared to the compressor rated cooling capacity, a maximum increase of 3% was recorded when the evaporator and condenser flowrates were maximum (Experiment 3). Nevertheless, the cooling capacity decreased for lower DIW flowrates in either the evaporator or the condenser (Experiments 5 and 8, respectively). This can be attributed to the decreased heat transfer caused by the evaporator pipe frosting at lower flowrates.

Fig. 9 illustrates the effect of changing the evaporator and condenser DIW flowrates on the compressor work. A considerable drop in compressor work was observed at higher evaporator and condenser DIW flowrates (Experiment 3). With the increase in evaporator and condenser DIW flowrates, there was a considerable decrease in superheated refrigerant temperature at the compressor outlet. Hence, the condenser pressure was reduced, and ultimately, the required compressor work was also reduced. A similar conclusion was reached by other researchers who performed similar studies [43]. By comparing the compressor work values in Fig. 9 with the rated compressor work of 47.3 kJ/kg, the double-pipe heat exchanger was effective in reducing the compressor work in all experimental configurations. A maximum compressor work reduction of 53% was recorded for the configuration with the highest DIW flowrate at both the evaporator and the condenser (Experiment 3). Parameshwaran and Kalaiselvam [44] used silver nanoparticles for a chiller system and concluded a maximum daily energy saving of 51%.

Fig. 10 shows the total electric current for each experimental configuration as measured by the Fluke energy analyzer. The figure shows the effect of changing the evaporator and condenser DIW flowrates on the operating electric current. When compared to the rated compressor current value, the total electric current decreased by an average of 20%. Experiment 3 recorded a 23% decrease in the maximum current, for which the DIW flowrate was maximum at both the evaporator and the condenser. As both the supply voltage and the power factor are constants, a decrease in current value indicates a reduction in the total power consumption of the air conditioning system.

The effect of changing the evaporator and condenser flowrates on the system COP is shown in Fig. 11. When comparing the typical rated compressor COP value of 4.9 with the experimentally obtained COP values, a maximum increase of 52.5% was achieved for Experiment 3. Rakesh and Manjunath [42] used a modified refrigeration system by incorporating a double-pipe heat exchanger in between the condenser and the expansion valve and reported a similar increase in the system COP by almost 50%. Balaji et al. [43] investigated the effect of integrating a shell-and-coil

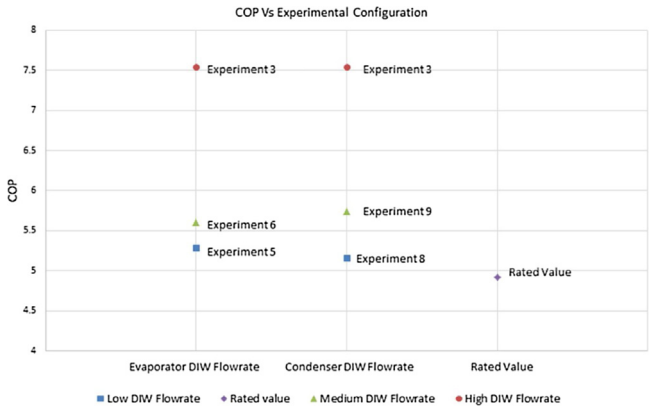

Fig. 11. COP versus experimental configuration.

type heat exchanger as an intercooler within a domestic air conditioning system and concluded a maximum COP enhancement of 49.32%.

As illustrated in Fig. 11, running DIW at lower flowrates at either the condenser or the evaporator did not considerably increase the overall system COP, whereas higher DIW flowrates increased the system COP (Experiments 9 and 6, respectively). It was also evident that the evaporator DIW flowrate had a greater impact on the overall system COP than the condenser DIW flowrate (Experiment 9).

4. Conclusion

This paper experimentally investigated the usage of double-pipe heat exchangers in domestic air conditioning applications. Double-pipe evaporator and condenser units were integrated in a vertical type air conditioning setup to study the feasibility of reducing compressor work and increasing the system COP. The unit was installed in a 45 m^3 balanced calorimeter of 2.24 kW heating load. Different evaporator and condenser DIW flowrates were used. Experimental results showed a considerable improvement in the system COP and power consumption when using double-pipe heat exchangers. A 3% maximum increase in the air conditioning unit cooling capacity was recorded. Increasing the DIW flowrates increased the system COP and improved the system power consumption. It was evident that the evaporator DIW flowrate had a greater impact on the overall system COP than the condenser DIW flowrate. In the best case, where the evaporator and the condenser DIW flowrates were at their maximum, a 53% reduction in the compressor work was recorded. The highest COP value was recorded for the same case with an enhancement of 52.5% in comparison to the rated standard compressor value. Compared to the compressor rated COP value, all the experiments in this study yielded a higher COP value. This work showed the potential for enhancing the performance of an air conditioning system by using double-pipe heat exchangers. Nevertheless, for an optimum thermal performance, attention should be given to several design aspects to avoid evaporator pipe frosting, thereby leading to a drop in the cooling capacity.

Acknowledgment

This publication was made possible by the NPRP award NPRP 6 - 461 - 2 – 188 from the Qatar National Research Fund (a member of The Qatar Foundation). The statements made herein are solely the responsibility of the authors.

References

[1] B.F. Yu, Z.B. Hu, M. Liu, H.L. Yang, Q.X. Kong, Y.H. Liu, Review of research on air-conditioning systems and indoor air quality control for human health, Int. J. Refrig. 32 (1) (2009) 3–20, http://dx.doi.org/10.1016/j.ijrefrig.2008.05.004.
[2] R. Qi, L. Lu, H. Yang, Investigation on air-conditioning load profile and energy consumption of desiccant cooling system for commercial buildings in Hong Kong, Energy Build. 49 (2012) 509–518, http://dx.doi.org/10.1016/j.enbuild.2012.02.051.
[3] R. Kosonen, F. Tan, Assessment of productivity loss in air-conditioned buildings using PMV index, Energy Build. 36 (2004) 987–993, http://dx.doi.org/10.1016/j.enbuild.2004.06.021.
[4] T. Kostiainen, I. Welling, M. Lahtinen, K. Salmi, E. Kähkönen, J. Lampinen, et al., Modeling of subjective responses to indoor air quality and thermal conditions in office buildings, HVAC&R Res. 9669 (May) (2016), http://dx.doi.org/10.1080/10789669.2008.10391046.
[5] S. Ghani, E.A. ElBialy, F. Bakochristou, S.M.A. Gamaledin, M.M. Rashwan, B. Hughes, Thermal performance of stadium's field of play in hot climates, Energy Build. 139 (2017) 702–718, http://dx.doi.org/10.1016/j.enbuild.2017.01.059.
[6] U.S. Energy Information Administration, International Energy Outlook 2016, vol. 0484, 2016 https://doi.org/www.eia.gov/forecasts/ieo/pdf/0484(2016).pdf.
[7] L. Perez-lombard, J. Ortiz, C. Pout, A review on buildings energy consumption information, Energy Build. 40 (2008) 394–398, http://dx.doi.org/10.1016/j.enbuild.2007.03.007.
[8] L. Pérez-lombard, J. Ortiz, J.F. Coronel, I.R. Maestre, A review of HVAC systems requirements in building energy regulations, Energy Build. 43 (2011) 255–268, http://dx.doi.org/10.1016/j.enbuild.2010.10.025.
[9] U.S. Energy Information Administration, Air Conditioning in Nearly 100 Million U.S. Homes, 2015.
[10] Z. Yang, B. Becerik-Gerber, The coupled effects of personalized occupancy profile based HVAC schedules and room reassignment on building energy use, Energy Build. 78 (2014) 113–122, http://dx.doi.org/10.1016/j.enbuild.2014.04.002.
[11] V. Vakiloroaya, B. Samali, A. Fakhar, K. Pishghadam, A review of different strategies for HVAC energy saving, Energy Convers. Manag. 77 (2014) 738–754, http://dx.doi.org/10.1016/j.enconman.2013.10.023.
[12] P. Promoppatum, S.C. Yao, T. Hultz, D. Agee, Experimental and numerical investigation of the cross-flow PCM heat exchanger for the energy saving of building HVAC, Energy Build. 138 (2017) 468–478, http://dx.doi.org/10.1016/j.enbuild.2016.12.043.
[13] Y.A. Cengel, M.A. Boles, Thermodyamics an engineering approach, Energy 1 (2007) 51, http://dx.doi.org/10.1017/CBO9781107415324.004.
[14] A. Bhatia, Design Options for HVAC Distribution Systems, vol. 877, 2012, pp. 68.
[15] AHRI 550/590, Standard for Performance Rating Of Water-Chilling and Heat Pump Water-Heating Packages Using the Vapor Compression Cycle, vol. 590, 2015, pp. 74.
[16] R. Prager, Chilled Water HVAC Systems, Brinco Mechanical Management Services, Inc., New York, 2012.
[17] Energy Design Resources, Chilled Water Plant Design Guide, 2009.
[18] S. Hanson, M. Schwedler, B. Bakkum, Chiller System Design and Control, 2011, Retrieved from http://www.tranebelgium.com/files/book-doc/12/fr/12.1hp13yp1.pdf.
[19] X. Fang, X. Jin, Z. Du, Y. Wang, The evaluation of operation performance of HVAC system based on the ideal operation level of system, Energy Build. 110 (2016) 330–344, http://dx.doi.org/10.1016/j.enbuild.2015.11.020.
[20] J. Park, S. Cho, S.K. Lee, S. Kang, Y.S. Kim, J.Y. Kim, D.S. Choi, Energy-saving decision making framework for HVAC with usage logs, Energy Build. 108 (2015) 346–357, http://dx.doi.org/10.1016/j.enbuild.2015.09.048.
[21] N. Targui, H. Kahalerras, Analysis of a double pipe heat exchanger performance by use of porous baffles and pulsating flow, Energy Convers. Manag. 76 (2013) 43–54, http://dx.doi.org/10.1016/j.enconman.2013.07.022.
[22] J.B. Williams, T. Walters, D. Hoon Han, Double-Pipe Heat Exchanger, 2002.
[23] S. Kakac, H. Lui, Heat Exchangers; Selection, Rating and Thermal Design, second edi., CRC Press, Florida, 2002.
[24] S. Kakaç, H. Liu, A. Pramuanjaroesnkij, Heat Exchangers: Selection, Rating, and Thermal Design, CRC Press, 2012.
[25] M. Omidi, M. Farhadi, M. Jafari, A comprehensive review on double pipe heat exchangers, Appl. Therm. Eng. 110 (2017) 1075–1090, http://dx.doi.org/10.1016/j.applthermaleng.2016.09.027.
[26] F.P. Incropera, D.P.D, Introduction to Heat Transfer (fourth), John Wiley and Sons, 2002.
[27] T. Ma, W.-x. Chu, X.-y. Xu, Y.-t. Chen, Q.-w. Wang, An experimental study on heat transfer between supercritical carbon dioxide and water near the pseudo-critical temperature in a double pipe heat exchanger, Int. J. Heat Mass Transf. 93 (2016) 379–387.
[28] M. Sheikholeslami, M. Jafaryar, F. Farkhadnia, M. Gorji-Bandpy, D.D. Ganji, Investigation of turbulent flow and heat transfer in an air to water double-pipe heat exchanger, Neural Comput. Appl. 26 (2015) 941–947.
[29] M. Sheikholeslami, M. Gorji-Bandpy, D. Ganji, Fluid flow and heat transfer in an air-to-water double-pipe heat exchanger, Eur. Phys. J. Plus 130 (2015) 1–12.
[30] X. Tang, X. Dai, D. Zhu, Experimental and numerical investigation of convective heat transfer and fluid flow in twisted spiral tube, Int. J. Heat Mass Transf. 90 (2015) 523–541.
[31] R. Bhadouriya, A. Agrawal, S. Prabhu, Experimental and numerical study of fluid flow and heat transfer in an annulus of inner twisted square duct and outer circular pipe, Int. J. Therm. Sci. 94 (96–109) (2015).

[32] H.S. Dizaji, S. Jafarmadar, F. Mobadersani, Experimental studies on heat transfer and pressure drop characteristics for new arrangements of corrugated tubes in a double pipe heat exchanger, Int. J. Therm. Sci. 96 (2015) 211–220, http://dx.doi.org/10.1016/j.ijthermalsci.2015.05.009.
[33] R. Raj, N.S. Lakshman, Y. Mukkamala, Single phase flow heat transfer and pressure drop measurements in doubly enhanced tubes, Int. J. Therm. Sci. 88 (2015) 215–227.
[34] N. Targui, H. Kahalerras, Analysis of a double pipe heat exchanger performance by use of porous baffles and nanofluids, World Acad. Sci. Eng. Technol. Int. J. Mech. Aerosp. Ind. Mechatron. Manuf. Eng. 8 (2014) 1590–1595.
[35] N. Targui, H. Kahalerras, Analysis of a double pipe heat exchanger performance by use of porous baffles and pulsating flow, Energy Convers. Manag. 76 (2013) 43–54.
[36] M. Sheikholeslami, M. Gorji-Bandpy, D. Ganji, Effect of discontinuous helical turbulators on heat transfer characteristics of double pipe water to air heat exchanger, Energy Convers. Manag. 118 (2016) 75–87.
[37] M. Sheikholeslami, M. Hatami, M. Jafaryar, F. Farkhadnia, D.D. Ganji, M.G.-Bandpy, Thermal management of double-pipe air to water heat exchanger, Energy Build. 88 (2015) 361–366.
[38] W.M. Rohsenow, J.R. Hartnett, Y. Cho, Handbook of Heat Transfer, 3rd ed., MCGRAW-HILL, 1998.
[39] H. Martin, Heat Exchangers, CRC Press, 1992.
[40] D. Kern, Process Heat Transfer, McGraw-Hill, 1950.
[41] S. Kakac, H. Liu, Heat Exchangers: Selection, Rating, and Thermal Design, CRC Press, Boca Raton, FL, 1998.
[42] R. Rakesh, H.N. Manjunath, Study of vapour compression refrigeration system using double pipe heat exchanger, Int. J. Adv. Res. Sci. Eng. (2016) 138–144.
[43] N. Balaji, P.S. Mohan, K.R. Velraj, Experimental investigations on the improvement of an air conditioning system with a nanofluid-based intercooler, Arab. J. Sci. Eng. (2015) 1681–1693, http://dx.doi.org/10.1007/s13369-015-1644-7.
[44] R. Parameshwaran, S. Kalaiselvam, Energy conservative air conditioning system using silver nano-based PCM thermal storage for modern buildings, Energy Build. 69 (2014) 202–212.
[45] Y.H. Yau, The use of a double heat pipe heat exchanger system for reducing energy consumption of treating ventilation air in an operating theatre-a full year energy consumption model simulation, Energy Build. 40 (5) (2008) 917–925, http://dx.doi.org/10.1016/j.enbuild.2007.07.006.
[46] ASHRAE. ASHRAE Standard 16 – Method of Testing for Rating Room Air Conditioners and Packaged Terminal Air Conditioners, 53(9), (2016) 1689–1699. doi: 10.1017/CBO9781107415324.004.
[47] AHRI, Performance Rating of Commercial and Industrial Unitary Air-Conditioning Condensing Units, 2015, pp. 365, January.
[48] ISO, International Standard ISO 5151, 2010.
[49] O. Alves, E. Monteiro, P. Brito, P. Romano, Measurement and classification of energy efficiency in HVAC systems, Energy Build. 130 (2016) 408–419, http://dx.doi.org/10.1016/j.enbuild.2016.08.070.
[50] Bureau of Standards Jamaica, Jamaican Standard Specification for Room Air Conditioner Energy & Other Performance Testing Notice, 2016, March.
[51] G. Cherem-Pereira, N. Mendes, Roomair conditioners: determination ofempirical Correlations for predicting building energy consumption, Eighth International IBPSA Conference (2003) 1017–1024.
[52] ANSI/ASHRAE, Standard 90. 2-2001 – Energy-Efficient Design of Low-Rise Residential Buildings, 2001.
[53] ASHRAE, 2001 ASHRAE Fundamentals Handbook (SI), (1984), 2001, pp. 8–13.